Available online at www.sciencedirect.com
SCIENCE DIRECT
Experimental Eye Research 79 (2004) 249–261
EXPERIMENTAL EYE RESEARCH
www.elsevier.com/locate/yexer

Cloning and characterization of a thermostable catfish αB-crystallin with chaperone-like activity at high temperatures

Chung-Ming Yu[a,c], Gu-Gang Chang[b], Hui-Chuan Chang[b], Shyh-Horng Chiou[c,d,*]

[a]*Graduate Institute of Life Sciences, National Defense Medical Center, Taipei, Taiwan*
[b]*Faculty of Life Sciences, Institute of Biochemistry, National Yang-Ming University, Taipei, Taiwan*
[c]*Laboratory of Crystallin Research, Institute of Biological Chemistry, Academia, Taipei, Taiwan*
[d]*Institute of Biochemical Sciences, National Taiwan University, P.O. Box 23-106, Taipei 10617, Taiwan*

Received 1 March 2004; accepted in revised form 7 April 2004

Abstract

We have cloned, expressed and characterized catfish αB-crystallin (FαB). Genomic sequence comparison has revealed conservation of intron splicing sites and coding regions, however, the two intron sequences, 5′- and 3′-untranslated regions of FαB gene are shorter than those reported for other vertebrates. In contrast to mammalian homologues with a subunit association ratio (αA-crystallin/αB-crystallin) of 3:1, α-crystallin from catfish lens showed a ratio of 19:1. The biophysical properties and chaperone-like activity of recombinant FαB and porcine αB-crystallin (PαB) were studied and compared by heat denaturation, circular dichroism, intrinsic and dye-binding fluorescence, gel-filtration, and analytical ultracentrifugation. FαB shows 50% precipitation occurring at 72°C that is higher than PαB at 66°C. Even though FαB also possesses more surface hydrophilic regions than PαB, FαB still possesses higher chaperone activity to prevent aggregation of alcohol dehydrogenase at 60°C. The molecular mass of FαB showed a smaller size (450 kDa) than PαB (550 kDa), which is also confirmed by analytical ultracentrifugation. In addition, FαB possesses better refolding potential after preheating treatment than PαB. FαB also exhibits higher chaperone-like activity than PαB to prevent insulin aggregation induced by dithiothreitol. In contrast to the prevalent notion that fish crystallins generally denature easily, FαB with chaperone-like activity appears to be more stable than mammalian homologues towards thermal and chemical denaturation.

Keywords: catfish eye lenses; αB-crystallin; thermostability; chaperone-like activity; small heat-shock protein; crystallin aggregation; surface hydrophilicity

1. Introduction

α-Crystallin constitutes a major class of lens proteins present in all vertebrate eye lenses (de Jong and Hendriks, 1986; Wistow and Piatigorsky, 1988). Native α-crystallin from mammalian lenses is commonly isolated as a large water-soluble aggregate with a molecular mass of about 600–800 kDa. It consists of two homologous subunits αA and αB of about 55–60% sequence identity (van der Ouderaa et al., 1973, 1974), each with a molecular mass of ~20 kDa and in a binding ratio (αA/αB) of 3:1 for most mammalian lenses (Groenen et al., 1994).

α-Crystallin was shown to possess structural and functional similarities to small heat-shock proteins (sHSP) (Ingolia and Craig, 1982; Hendrick and Hartl, 1993). These proteins were first sequenced for sHSP isolated from Drosophila (Ingolia and Craig, 1982) and found to contain a highly conserved region strikingly similar to the C-terminal two-thirds of α-crystallin sequence, now denoted as α-crystallin domain (Ingolia and Craig, 1982; Wistow, 1985). The role of this conserved region was first suggested to be a highly stable structural unit or a useful building block for proteins under stressful environments (Wistow, 1985). However, in vitro studies of α-crystallin indicated a chaperone-like activity associated with this lens

Abbreviations: ADH, alcohol dehydrogenase; ANS, 1-anilinonaphthalene-8-sulfonic acid; CD, circular dichroism; FαB, catfish αB-crystallin; HPLC, high performance liquid chromatography; PBS, phosphate buffered saline; PCR, polymerase chain reaction; PαB, porcine αB-crystallin; RT-PCR, reverse transcription coupled polymerase chain reaction; sHSP, small heat-shock protein; UTR, untranslated regions.

* Corresponding author. Address: Dr Shyh-Horng Chiou, Institute of Biochemical Sciences, National Taiwan University, P.O. Box 23-106, Taipei 10617, Taiwan, ROC.
E-mail address: shchiou@gate.sinica.edu.tw (S.-H. Chiou).

0014-4835/$ - see front matter © 2004 Elsevier Ltd. All rights reserved.
DOI:10.1016/j.exer.2004.04.006

protein (Horwitz, 1992), which raises the supposition that α-crystallin is essential not only for the structural integrity required for lens transparency, but also for its chaperone-like role in maintaining the solubility of other lens proteins (Horwitz, 1993).

αB-Crystallin has been shown to be expressed in other tissues besides the lens suggesting that it may possess a general cellular function (Ingolia and Craig, 1982; Hendrick and Hartl, 1993). However, zebrafish αB-crystallin is expressed at extremely low levels outside of the lens (Posner et al., 1999). Expression of αB-crystallin was shown to confer protection to cells against thermal (Horwitz, 1992), osmotic (Golenhofen et al., 2002), and oxidative injuries (Klemenz et al., 1991). Most significantly relating to physiological functions is the finding that outside the lens tissue the R120G mutation of αB-crystallin can directly account for inheritable desmin-related myopathies (Vicart et al., 1998). Interestingly, αB-crystallin is also found to be overexpressed in many neurological disorders such as Creutzfeldt–Jacob disease (Renkawek et al., 1992), Alzheimer's disease (Renkawek et al., 1994), diffuse Lewy body disease (Jackson et al., 1995), and Alexander's disease (Iwaki et al., 1989). All the available data attest to the general functional significance of αB-crystallin.

Fish represents the oldest and most diverse group of vertebrates (Powers, 1989). The modern fishes comprise two major classes of piscine species, i.e. *Osteichthyes* or teleostean (bony) fishes, and *Chondrichthyes* or cartilaginous fishes (sharks and skates). The study of lens crystallins from the piscine class is of special interest from the evolutionary point of view because they constitute the early protein forms of vertebrates and are thought to be ancestral to those of land vertebrates. It is especially noteworthy that the abundant presence of various common and specific classes of structurally conserved crystallins in eye lenses of different species of vertebrates constitutes a good model system to unravel the complex process of evolution in structurally homologous proteins (Chiou, 1986; de Jong and Hendriks, 1986). Catfishes reside generally in the dark or underground environment, belonging to species of nocturnal scavengers. They thus constitute a rare species in vertebrates to study the evolutionary effects on the structure and function of αB-crystallin. We have characterized here the structural difference of αB-crystallins between catfish and other vertebrates on the genomic DNA and protein levels. Because the porcine αB-crystallin (PαB) possesses similar biophysical properties and chaperone-like activity to the well-studied αB-crystallins from human and bovine species in our previous studies (Liao et al., 2002b), we have tried to characterize the differences between biophysical properties and chaperone-like activity of catfish αB-crystallin (FαB) and PαB. Several important differences were found between αB-crystallins from catfish and porcine lenses, which may point out some important aspects of this sHSP in regard to its interactions with other crystallins and its function in the lens.

2. Materials and methods

2.1. Materials

Equine liver alcohol dehydrogenase (ADH) was obtained from Sigma. γ-Crystallin was obtained from porcine eye lenses. All restriction enzymes were purchased from New England Biolabs. 1-Anilinonaphthalene-8-sulfonic acid (ANS) was purchased from Molecular Probes.

2.2. Preparation of mRNA and intron sequence analysis of FαB

Total RNA of catfish lenses was purified using the *TRIZOL* reagent (Invitrogen) following the protocol from the manufacturer. The 5′- and 3′-untranslated region (UTR) sequences were determined by the protocols from SMART Race cDNA amplification system (Clontech, BD Biosciences). The chromosomal DNA of catfish used in intron sequence determination was prepared according to the protocols of *TRIZOL* reagent after total RNA preparation. The first and second introns of FαB gene were amplified from catfish chromosome DNA by using two primer pairs based on the exon sequences covering the first and second introns of FαB gene. These polymerase chain reaction (PCR) products were cloned with *p*GEM-Teasy vector (Promega) for sequencing.

2.3. Construction and expression of cDNA clones for FαB and PαB

The coding region for FαB gene was amplified from catfish lens cDNA mixture and subcloned into pET21b expression vector (Novagen) with *Nde* I and *Hind* III cutting sites. Expression clone of PαB was constructed as described previously (Liao et al., 1998).

FαB and PαB were expressed in *Escherichia coli* BL21 (DE3) cells and purified by the methods described previously (Liao et al., 1998) with some modifications for FαB expression and purification. Because the recombinant FαB after gel-filtration analysis was easily precipitated in 50% acetonitrile used in the reverse-phase high-performance liquid chromatography (HPLC) system, the precipitates containing FαB were centrifuged at 300 × *g* for 10 min and washed once with 100% acetonitrile. The FαB precipitates could be dissolved in acidic ddH_2O (0·1% TFA). The lyophilized recombinant FαB or PαB was dissolved in phosphate-buffered saline (PBS) with 8 M urea and introduced to TSK HW-55 gel-filtration column for protein refolding and renaturation. The fractions containing purified FαB or PαB were pooled and concentrated by VIVASPIN Concentrator (100 kDa molecular-mass cut-off, Vivascience). The protein concentrations were determined by absorbance measurements using extinction coefficients calculated from amino acid sequence data of each protein (Gill and von Hippel, 1989). These purified proteins were

stored at 4 or −20°C for short or long term storage, respectively.

2.4. Thermal stability analysis

Temperature-dependent aggregation of FαB and PαB were monitored in Ultraspec 4000 UV/VIS spectrophotometer equipped with a Peltier type temperature controller (Amersham Pharmacia). The heating rate was 1°C min^{-1}. The temperature range for protein heating treatment was from 25 to 95°C. The protein aggregation was monitored by light scattering at 360 nm. Protein concentration used was 0·7 mg ml^{-1} in PBS. First derivative calculation was used to estimate the temperature at which 50% precipitation had occurred.

2.5. Circular dichroism spectra analysis

Circular dichroism (CD) spectra were performed on a JASCO J-715 spectropolarimeter. The temperatures for CD measurement were controlled and maintained by a thermostatic, circulating water bath. The far-UV CD spectra were recorded as the mean of 5 accumulations with a 0·02 cm path length water-jacket cell from 250 to 190 nm and the near-UV CD spectra as the mean of 10 accumulations with a 1 cm path length water-jacket cell from 360 to 250 nm under constant N_2 flush and constant-temperature water flow. All CD spectra were corrected for their respective buffer blanks. Spectra were also noise-reduced by polynomial curve fitting program supplied by the manufacturer, with the precaution of not over-smoothing the data points. The CD data were expressed as molar ellipticity in $[\theta]$ (degrees cm^2 $dmol^{-1}$). The wavelength scan data was recorded in 0·2 nm steps with 1·0 nm bandwidth, 50 nm min^{-1} scanning speed and 2 sec response time. Protein concentrations used in both CD spectra were 0·7 mg ml^{-1} in 10 mM phosphate buffer, pH 7·4.

2.6. Fluorescence measurements

Intrinsic and ANS-binding fluorescence were recorded by an F4500 fluorescence spectrophotometer (Hitachi) with circulating water bath to maintain desired temperatures. The cuvette with a 0·3 cm × 0·3 cm cross section and 60 μl of protein sample each were used for measurements. The intrinsic fluorescence of Trp residues was measured with an excitation wavelength at 295 nm. ANS was used to determine the surface hydrophobicity of protein molecule (Johnson et al., 1979) and measured with an excitation wavelength at 395 nm. To determine the temperature-dependent changes of Trp intrinsic and ANS-binding fluorescence, the equilibrium time of protein samples for each specified temperature was 30 min in a thermostatic controller before measurements. The protein concentration used was 100 μg ml^{-1} in PBS. ANS solution (10 μl of 10 mM stock solution) was thoroughly mixed with 1 ml protein samples, incubated for 5 min at specified temperatures to establish equilibrium. The emission spectra were recorded from 300 to 400 nm and from 400 to 600 nm for the Trp intrinsic and ANS-binding fluorescence measurements, respectively. The excitation and emission bandwidth were set at 5 nm. All quantum yields of fluorescence spectra were corrected for their respective buffer blanks or ANS only at different temperatures.

2.7. Gel-permeation FPLC analysis

Multimeric sizes of recombinant FαB and PαB were evaluated by an analytical Superose-6 HR 10/30 column with FPLC system (Amersham Pharmarcia). Molecular-weight standards for gel-filtration (Sigma) were used for calibration. The protein concentration used was 1 mg ml^{-1} in PBS and 0·4 ml sample was auto-injected. The column was eluted at 0·4 ml min^{-1} with PBS. All samples were passed through the syringe-driven filter (pore size 0·45 μm) before analysis. The width-of-half-height of each sample was determined by the program equipped in FPLC system and used to estimate the polydisperse property of FαB and PαB.

2.8. Analytical ultracentrifugation analysis

The molar-mass distribution of FαB and PαB under various preheating treatments was estimated by a Beckman-Coulter XL-A analytical ultracentrifuge with an An60Ti rotor. Sedimentation velocity was performed at 20°C and 25 000 rpm with standard double sectors aluminium centrepieces. The UV absorption of the cells was scanned every 5 min for 2 h. The data were analyzed with the SedFit program (Schuck, 2000). The solvent density and viscosity were corrected with the UltraScan version 5·0 (Demeler and Saber, 1998). A partial specific volume of 0·705 and 0·718 were used for FαB and PαB, respectively (Harpaz et al., 1994). All samples were visually checked for clarity after ultracentrifugation. The protein concentration used was 1 mg ml^{-1} in PBS.

2.9. Chaperone-like activity assay

Chaperone-like activities of FαB and PαB were analyzed by measuring the capability to prevent the aggregation of ADH denatured by heating treatment or the reduction of disulfide bonds in insulin. The aggregation assays with different substrate proteins were performed essentially as described previously (Horwitz et al., 1998a). The extent of aggregation was measured as a function of time by monitoring the light scattering at 360 nm in a Pharmacia F-4000 fluorescence spectrophotometer with Peltier type controller and recorded at 1-s intervals. The aggregations of ADH (0·4 mg ml^{-1}) in PBS with FαB or PαB in a molar ratio of 2:1 (ADH/αB-crystallin) were monitored at 50 and 60°C. The dithiothreitol (DTT)-induced aggregation of

insulin (0·4 mg ml^{-1}) in PBS was studied at 25 and 37°C with various molar ratios of insulin to FαB or PαB. The suppression of aggregation was calculated by the percent (%) change of absorbance at 360 nm in the absence and presence of αB-crystallins.

3. Results and discussion

3.1. Genomic structure of FαB gene

Our recent interest has been focused on one teleostean species, i.e. the catfish, a nocturnal scavenger which is commonly raised in the local aquacultures of Taiwan. We have amplified cDNAs constructed from the lenses of catfishes by PCR methodology in order to aid in the genomic analysis of the major eye lens protein with chaperone-like function, i.e. α-crystallin consisting of αA- and αB-crystallin subunits. Important insights into the evolutionary history of different protein families are being discovered through the analysis of molecular sequences.

The FαB gene encodes a protein of 172 amino acids in length. The genomic structure and all intron/exon boundaries of αB-crystallins reported for vertebrate species including catfish are conserved. The three exons of FαB gene code for residues 1–64, 65–105, and 106–172 of FαB protein sequence, respectively. The first and second introns are located between position 70 and 71, and between position 111 and 112, respectively, of the alignment in Fig. 1. However, the lengths of the two intron sequences of FαB gene (375 and 111 bps in length, respectively) were much shorter than the homologues from other vertebrates (Table 1). The 5′ and 3′-UTR sequences of FαB gene were also found slightly shorter than homologous sequences from other vertebrates (Table 1). The general observation in genomic analysis is that more complex organisms generally have more introns with longer lengths (Logsdon, 1998). The numbers of protein-coding genes do not increase exponentially in complex organisms according to the results of genome projects currently established (Chervitz et al., 1998; Roest Crollius et al., 2000; Rubin et al., 2000), but the intron density, size and sequence complexity correlate well with their developmental complexity (Mattick and Gagen, 2001). The gene and protein sequence comparison shown for αB-crystallins below seem to indicate that catfish belongs to fishes of ancient evolutionary status.

3.2. Protein sequence alignment and comparison

Based on conserved domain homology search by blastp module in BLAST server (http://www.ncbi.nlm.nih.gov/blast), FαB, which is similar to its homologues, could be separated into three distinct structural domains, the N-terminal domain (residues 1–59, which was three amino acids shorter than PαB), C-terminal α-crystallin domain (residues 60–159) and C-terminal extension (residues 160–172).

FαB shows high sequence similarity with other vertebrate species based on protein sequence alignment. Protein sequence alignment of FαB with other vertebrate homologues is analyzed by CLUSTAL V program (Higgins et al., 1991) in the MegAlign module of Lasergene package (DNASTAR, Inc., Madison, WI, USA) (Fig. 1). A distinct gap was introduced between residues #44 (valine) and #45 (tyrosine) of FαB, which corresponded to a conserved SPF (Ser-Pro-Phe) tripeptide in the sequences of other vertebrates except zebrafish. This tripeptide contains a Ser residue that could be phosphorylated in vivo (Chiesa et al., 1987). Another conserved Ser residue at position 19 in mammalian αB-crystallins was absent in FαB, which was also found to be lost in zebrafish αB-crystallin (Posner et al., 1999). The Ser residue at position 62 of the alignment in Fig. 1 is conserved in all vertebrate αB-crystallins, which was also shown to be phosphorylated in vivo (Chiesa et al., 1987). However, the physiological significance of phosphorylation at these conserved serine residues remains unknown. It does not appear to play some essential role in chaperone-like activity as judged by the substitution or lack of serine residues in FαB.

Table 2 summarizes the basic parameters obtained by comparison of protein sequences of αB-crystallins from catfish and other vertebrates. It is noteworthy that W9 was conserved in all vertebrates except birds. The most conserved Trp residue was located at position 63 of the alignment in Fig. 1. In addition, another conserved Tyr residue was located at position 125 of the alignment in Fig. 1. The estimated molar extinction coefficient (ε_{280}) of FαB based on amino acid contents (Gill and von Hippel, 1989) was 27 880 M^{-1} cm^{-1} which is two times higher than those of mammalian vertebrates (13 940 M^{-1} cm^{-1}) because of its high Trp content (4 versus 2 residues per molecule). In addition, zebrafish possesses the highest ε_{280} (33 000 M^{-1} cm^{-1}) due to the highest content of Tyr residues. Note that all Trp residues found in αB-crystallins are located at the N-terminal domain (Fig. 1). In general, the estimated p*I* values of mammals were higher than birds and fishes. The contribution of these conserved Trp and Tyr residues to the structure and chaperone-like activity of αB-crystallin is unknown; however, these residues could be good targets for site-specific mutagenesis in biophysical studies (Liang et al., 1999).

The systematic pair-wise protein sequence comparison of FαB and 12 homologous αB-crystallin sequences from four major classes of vertebrates as templates for the construction of a phylogenetic tree were performed by using a combination of distance matrix and approximate parsimony methods (Hein, 1990) (Fig. 2). It is noteworthy that the phylogenetic tree based on the sequence divergence among these protein sequences indeed exemplifies the dissimilarity between piscine αB-crystallins (e.g. catfish, dogfish and zebrafish) and other terrestrial vertebrate species (Fig. 2).

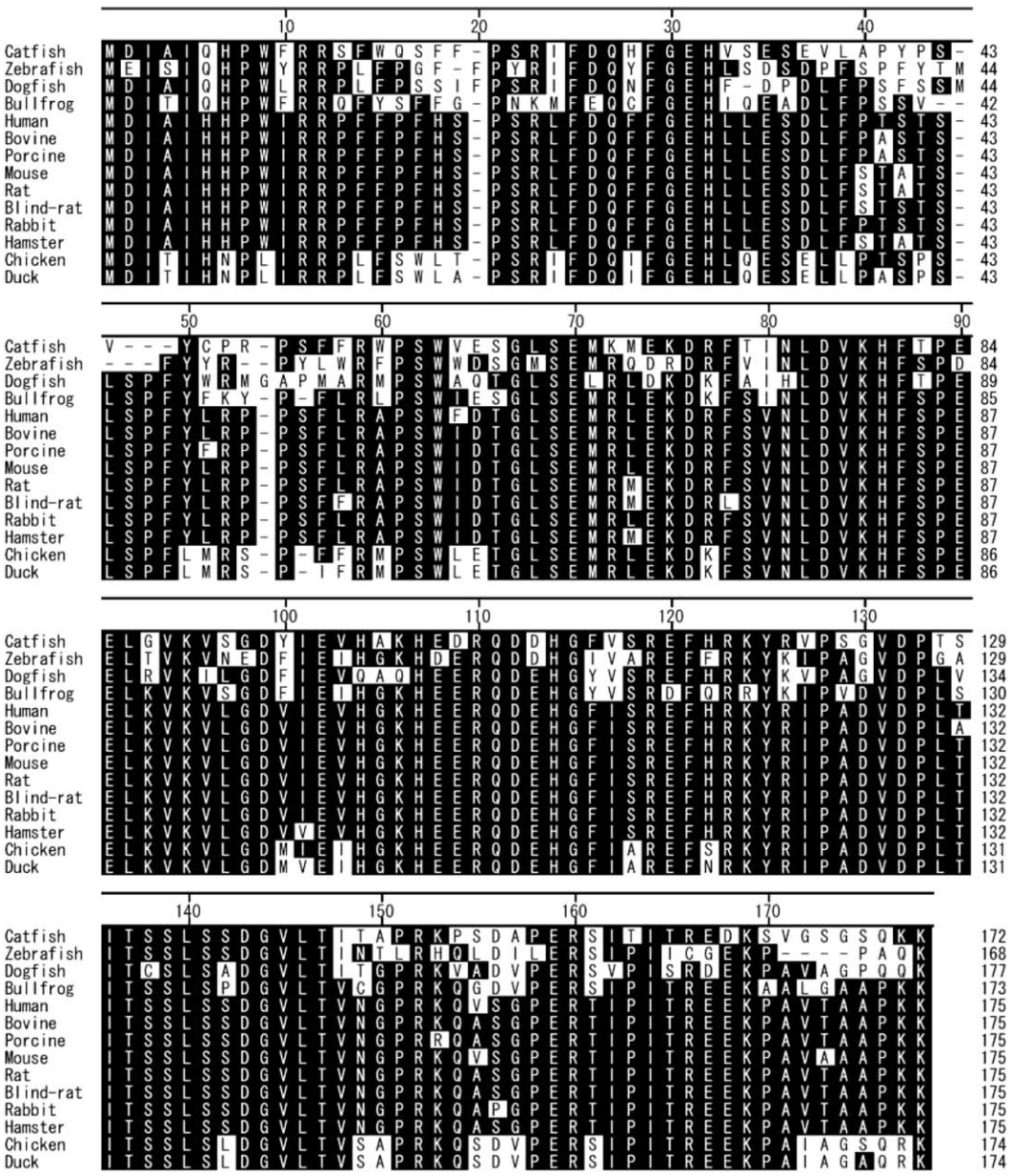

Fig. 1. Multiple sequence alignment of 13 αB-crystallin protein sequences from species of different vertebrate classes. The identical amino acid residues among various sequences based on the first one (catfish) are shaded in black blocks. The gaps denoted in dashes were introduced for optimal alignment and maximum homology for the aligned sequences. The splicing sites of αB-crystallins are conserved and the first and second introns are located between position 70 and 71, and between position 111 and 112, respectively. These αB-crystallin sequences shown are from catfish (*Clarias batrachus*), zebrafish (*Danio rerio*), spiny dogfish (*Squalus acanthias*), bullfrog (*Rana catesbeiana*), human (*Homo sapiens*), bovine (*Bos taurus*), porcine (*Sus scrofa*), mouse (*Mus musculus*), rat (*Rattus norvegicus*), blind rat (*Spalax judaei*), rabbit (*Oryctolagus cuniculus*), golden hamster (*Mesocricetus auratus*), chicken (*Gallus gallus*), and duck (*Anas platyrhynchos*) in GenBank. Amino acid residues are denoted by one-letter symbols.

The surface hydrophilicity analysis for the distribution of amino acids along primary protein sequences of FαB and PαB was analyzed (Fig. 3). The mean Kyte–Doolittle hydropathy of the polypeptide (Kyte and Doolittle, 1982) of FαB possessed higher hydrophilic content (0·7) than that of PαB (0·5), especially in the N-terminal segment (0·4 and 0·1 for FαB and PαB, respectively) and C-terminal extension region (1·2 and 0·7 for FαB and PαB, respectively). In addition, FαB also appears to possess a more hydrophilic α-crystallin domain than PαB (0·8 versus 0·7).

Table 1
The length of non-coding regions of αB-crystallin in different genomic sequences from various vertebrates (from GenBank)

Accession number	Species	Intron I (bp)	Intron II (bp)	5′-UTR (bp)	3′-UTR (bp)
M73741	Mouse	1048	1656	475	138
U04320	Rat	1020	1981	44	653
U16124	Duck	1492	1111	39	702
AY184812	Catfish	375	111	29	31

Table 2
Comparison of basic parameters based on protein sequences of αB-crystallins from catfish and other vertebrates

	Trp (W) content and position	Estimated extinction coefficient (ε_{280}) (M^{-1} cm^{-1})	Protein length	Estimated p*I*	Molecular weight	Tyr (Y) content and position
Zebrafish	4 (W9, W52, W57, W58)	33 000	168	5·77	19977·5	8 (Y10, Y21, Y27, Y42, Y46, Y47, Y50, Y119)
Catfish	4 (W9, W15, W54, W57)	27 880	172	6·44	19831·1	4 (Y41, Y45, Y94, Y119)
Dogfish	3 (W9, W50, W62)	20 910	177	6·38	20254·1	3 (Y49, Y115, Y124)
Bullfrog	2 (W9, W58)	17 900	173	6·31	20078·8	5 (Y15, Y47, Y50, Y111, Y120)
Chicken	2 (W17, W59)	12 660	174	6·31	20019·9	1 (Y121)
Porcine	2 (W9, W60)	13 940	175	6·76	20128·8	2 (Y48, Y122)
Human	2 (W9, W60)	13 940	175	6·76	20158·9	2 (Y48, Y122)

The basic parameters were obtained from the analysis by using the ExPASy server with ProtParam tool.

The comparison points to the fact that FαB is more hydrophilic than PαB, resulting in a higher solubility of FαB compared to PαB especially at high temperatures (see below).

3.3. Expression and purification of catfish αB-crystallin

The gel-filtration of lens crystallins from catfish showed that there were three major peaks (data not shown), which is

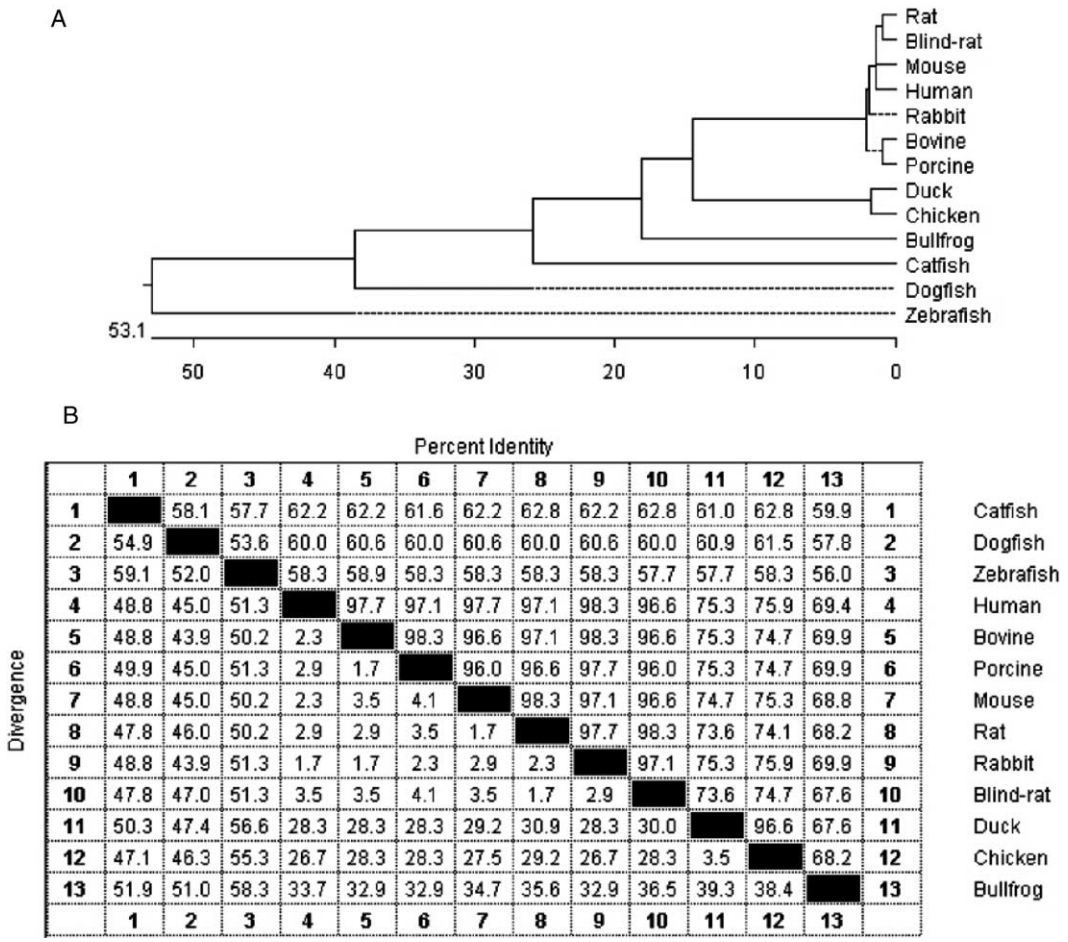

	1	2	3	4	5	6	7	8	9	10	11	12	13	
1		58.1	57.7	62.2	62.2	61.6	62.2	62.8	62.2	62.8	61.0	62.8	59.9	1
2	54.9		53.6	60.0	60.6	60.0	60.6	60.0	60.6	60.0	60.9	61.5	57.8	2
3	59.1	52.0		58.3	58.9	58.3	58.3	58.3	58.3	57.7	57.7	58.3	56.0	3
4	48.8	45.0	51.3		97.7	97.1	97.7	97.1	98.3	96.6	75.3	75.9	69.4	4
5	48.8	43.9	50.2	2.3		98.3	96.6	97.1	98.3	96.6	75.3	74.7	69.9	5
6	49.9	45.0	51.3	2.9	1.7		96.0	96.6	97.7	96.0	75.3	74.7	69.9	6
7	48.8	45.0	50.2	2.3	3.5	4.1		98.3	97.1	96.6	74.7	75.3	68.8	7
8	47.8	46.0	50.2	2.9	2.9	3.5	1.7		97.7	98.3	73.6	74.1	68.2	8
9	48.8	43.9	51.3	1.7	1.7	2.3	2.9	2.3		97.1	75.3	75.9	69.9	9
10	47.8	47.0	51.3	3.5	3.5	4.1	3.5	1.7	2.9		73.6	74.7	67.6	10
11	50.3	47.4	56.6	28.3	28.3	28.3	29.2	30.9	28.3	30.0		96.6	67.6	11
12	47.1	46.3	55.3	26.7	28.3	28.3	27.5	29.2	26.7	28.3	3.5		68.2	12
13	51.9	51.0	58.3	33.7	32.9	32.9	34.7	35.6	32.9	36.5	39.3	38.4		13
	1	2	3	4	5	6	7	8	9	10	11	12	13	

Fig. 2. Phylogenetic tree of 13 αB-crystallins from species of different vertebrates classes based on protein sequences. Analysis of sequence data was carried out in MegAlign program module in Lasergene package (DNASTAR, Inc., Madison, WI, USA). The percent divergence is calculated by comparing sequence pairs in relation to the relative positions in the phylogenetic tree, in contrast to the percent identity, which is estimated by comparing percent sequence identity directly without accounting for phylogenetic relationships. A phylogenetic tree (A) was then constructed based on the percent divergence (B) between protein sequences using a combination of distance matrix and approximate parsimony methods in the phylogeny generation program of Hein (1990). The tree was built using the CLUSTAL V program and weighted residue-weight table. The length in each branch represents the sequence distance between aligned pairs. The scale beneath the tree measures the distance between sequences (in millions of years). The dotted lines shown in (A) point to the fact that the sequence distance based on protein sequence comparison is not proportional to the scale.

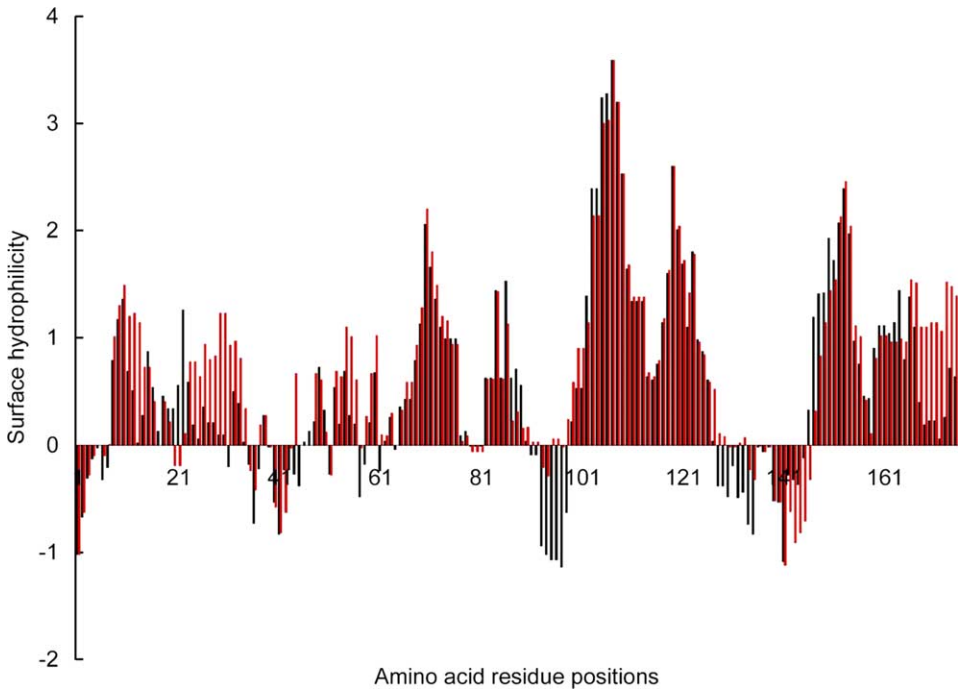

Fig. 3. Hydrophilicity analysis of FαB (red column) and PαB (black column). The hydrophilicity plots of FαB and PαB were performed by using Protean module in Lasergene package (DNASTAR, Inc., Madison, WI, USA). The hydrophilicity scores shown in the plot (window size = 9 amino acids) were based on the hydrophilic properties of amino acid residues in the protein primary sequence, higher positive scores indicating more hydrophilic. Three blank spaces were inserted to FαB protein sequence between V44 and Y45 in order to fill up the gap between the sequence alignments of the two αB-crystallins.

similar to our previous studies in carp (Chiou et al., 1986). α-Crystallin from catfish lenses was shown to co-elute with β-crystallins (Fig. 4, Lane 3), similar to our previous study for carp α-crystallin (Chiou et al., 1986). However, the ratio of αA and αB subunits of catfish α-crystallin was found to be about 19:1 by densitometric analysis (Scion Image beta 4·02 for Win, Scion Co., Frederick, Maryland, USA) on the SDS-PAGE of the fractions containing catfish α-crystallin, whereas a ratio of 3:1 was found in all mammalian homologues (Groenen et al., 1994). Because of the low abundance of FαB in catfish lens, we could not obtain enough proteins for detailed structural and functional analyses. Therefore, we construct the recombinant FαB for biophysical and chaperone-like activity assays. It is noted that catfish αA-crystallin could not be refolded after denaturation, which hampered its isolation and purification by C4 reverse phase HPLC system used for mammalian αA-crystallin purification and characterization (Perry and Abraham, 1986). The purification of recombinant catfish αA-crystallin will be reported later using another protocol described by Merck et al. (1992).

FαB was overexpressed in *E. coli* with an apparent molecular mass of 20 kDa (Fig. 4, Lane 1). The purity of recombinant FαB from reversed-phase HPLC was shown to be higher than 99% (Fig. 4, Lane 2). Analysis by mass spectrometry (19 831·6 Da) also confirmed its correct molecular mass (19 831·1 Da from sequence). It is noted that the lyophilized FαB from reversed-phase HPLC can be dissolved in 8 M urea and refolded by gel-filtration chromatography to get a multimeric homoaggregate of about 450 kDa.

3.4. Comparison of thermal stability

In order to compare the difference of thermostability, the aggregation of FαB and PαB was monitored by light scattering at 360 nm (Fig. 5) from 25 to 85°C. The PαB did

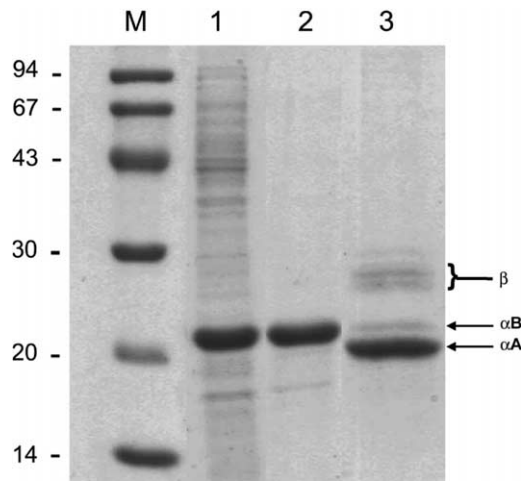

Fig. 4. SDS-PAGE analysis of recombinant FαB and native catfish lens α-crystallin. Lane 1, overexpressed crude lysate of recombinant FαB; Lane 2, purified recombinant FαB; Lane 3, α-crystallin fraction isolated from lenses. The arrows indicate αA and αB subunits of FαB. The included region with character '}' indicates the β-crystallins associated with catfish lens α-crystallin. The ratio of αA/αB is about 19:1, which is dramatically different from 3:1 for most mammalian α-crystallin. Standard protein markers (in kDa) are shown on the left lane: phosphorylase b (94), bovine serum albumin (67), ovalbumin (43), carbonic anhydrase (30), soybean trypsin inhibitor (20), and lysozyme (14).

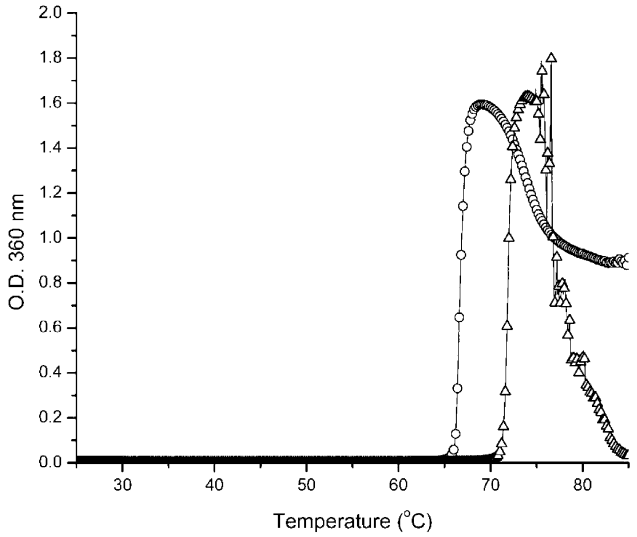

Fig. 5. Temperature stability of FαB and PαB. (A) Thermal stability of recombinant FαB (△) and PαB (○). Temperatures at 50% precipitation during heating process were calculated to be 66 and 72°C for PαB and FαB, respectively.

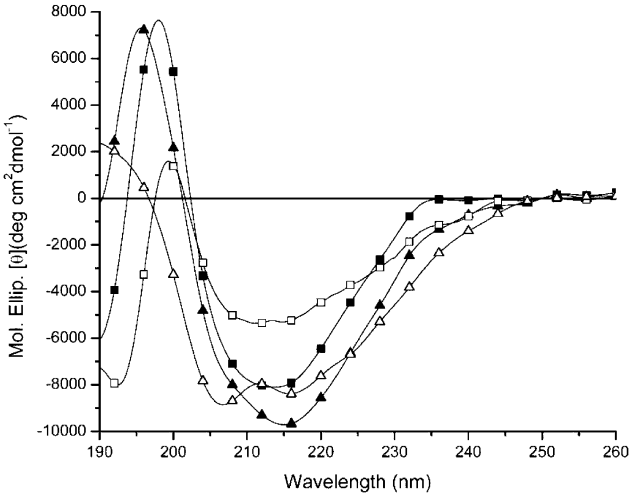

Fig. 6. The far-UV CD spectra of FαB and PαB at different temperatures. (■), FαB at 25°C; (□), PαB at 25°C; (▲), FαB at 60°C; (△), PαB at 60°C. Note that PαB at 60°C shows partially unfolded structure with CD minimum shifting to 207 nm, indicating a loss of β-sheet structure.

not aggregate up to 65°C with a 50% precipitation occurring at 66°C, whereas the FαB remained soluble up to 70°C and showed a 50% precipitation occurring at 72°C (Fig. 5). These results suggested that the thermostability of FαB was higher than those of PαB. The temperature for 50% aggregate formation of PαB is similar to that of human αB-crystallin (64·5°C), which has been found to correlate with the structural transition temperature in far-UV CD analysis (Perng et al., 1999).

3.5. Comparison of secondary and tertiary structures

Far-UV CD can be used to estimate secondary structure contents, whereas near-UV CD can be used to monitor the microenvironments of aromatic amino acids present in native proteins (Dinner et al., 2000). The far- and near-UV CD spectra measured with temperature and wavelength scan of FαB and PαB were used to compare the structural difference between these two proteins (Fig. 6). The wavelength scan CD spectra in the far- and near-UV ranges of FαB and PαB showed that the molar ellipticity of each spectrum decreased at elevated temperatures (Fig. 6 and data not shown for near-UV CD). Secondary-structure estimation based on far-UV CD spectra for FαB and PαB under various temperatures were analyzed by SELCON 3 (Sreerama et al., 1999) in the CDPro package. FαB contained higher molar ellipticity (more negative) and higher β-sheet content (32%) than PαB (28%) at 25°C (Fig. 6). These results are also consistent with the prevailing evidence that α-crystallin possesses mostly β-sheet secondary structures (Bloemendal et al., 1999). PαB contains twice as much random coil conformations (44%) than FαB (22%) at 60°C. However, FαB possesses more β-sheet structure at 60°C (42%) than at 25°C (32%). These data also suggested that FαB is more thermostable than PαB.

3.6. Intrinsic tryptophan fluorescence spectra and surface hydrophobicity

The intrinsic fluorescence of Trp residue can provide useful information of the conformational changes within a protein. The emission wavelength maxima (Trp λ_{max}) and fluorescence intensity at emission wavelength maxima (I_{Trp}) were recorded to compare the conformational difference between FαB and PαB. Because FαB and PαB possess 4 and 2 Trp residues in the N-terminal segment, it is not surprising to find that the I_{Trp} of FαB is higher than PαB at 25°C; however, the I_{Trp} of FαB was lower than PαB at 60°C (Fig. 7(A)). The Trp λ_{max} of FαB showed no significant changes from 25 (340·8 nm) to 60°C (341·4 nm), however, the Trp λ_{max} of PαB are significantly red-shifted from 25 (338·8 nm) to 60°C (344·5 nm) (Fig. 7(A)). The change (in intensity) observed in FαB upon heating to 60°C is probably due to a local displacement of a quenching group, since no corresponding conformational change is observed in CD (Fig. 6), while the redshift in the Trp λ_{max} of PαB shows that its unfolding transition already commences at 60°C, which is also corroborated by CD (Fig. 6).

We have also used ANS as an environmentally sensitive fluorophore to probe the surface hydrophobicity differences in FαB and PαB under different temperatures. The emission wavelength maxima (ANS λ_{max}) and fluorescence intensity at emission wavelength maxima (I_{ANS}) were recorded to compare the surface hydrophobicity difference between FαB and PαB. PαB showed not only higher I_{ANS} but also smaller ANS λ_{max} than FαB at different temperatures (Fig. 7(B)). It suggests that PαB possesses more hydrophobic surface than FαB at temperatures below 60°C.

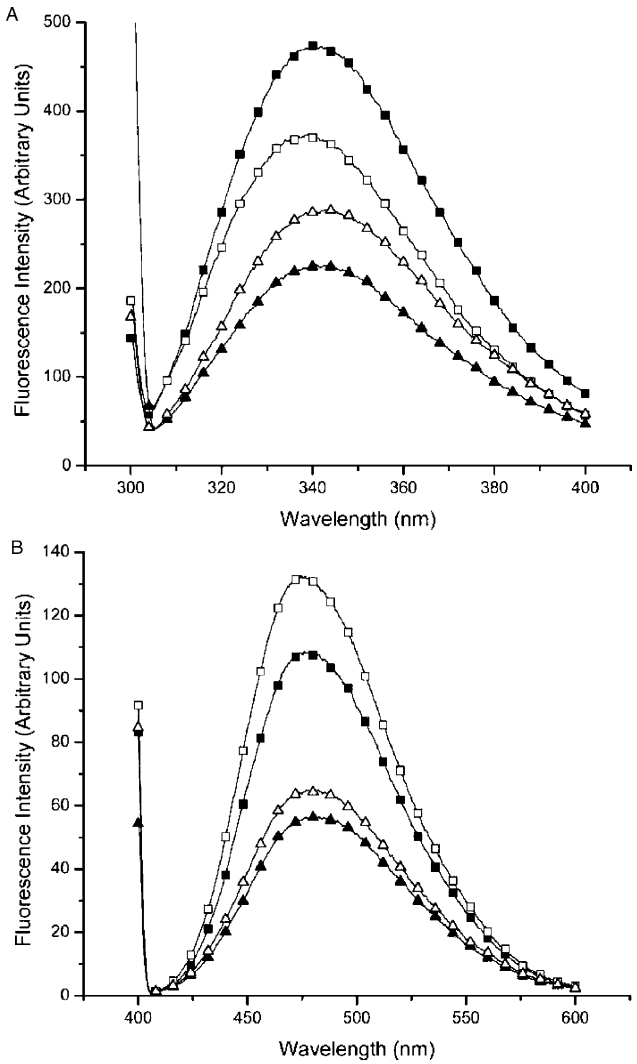

Fig. 7. Intrinsic tryptophen (Trp) and ANS-binding fluorescence spectra of FαB and PαB. (A) The intrinsic Trp fluorescence spectra of FαB at 25 (■) and 60°C (▲), and PαB at 25 (□) and 60°C (△). The greater decrease of Trp intrinsic fluorescence in FαB as compared to PαB at 60°C is probably due to higher exposure of Trp residues to solvent by its higher surface hydrophilicity. (B) The ANS-binding fluorescence spectra of FαB at 25 (■) and 60°C (▲), and PαB at 25 (□) and 60°C (△). Note that ANS-binding fluorescence is lower for FαB than PαB at 60°C, even though FαB possesses higher chaperone-like activity at 60°C than PαB.

The ANS λ_{max} of FαB and PαB were both slightly red-shifted from 25 to 60°C and the I_{ANS} also showed temperature dependent decrease in both αB-crystallins (Fig. 7(B)). These data appeared to suggest that FαB exposed much less hydrophobic regions, which is consistent with the predicted results of hydrophilicity analysis (Fig. 3).

3.7. Analytical gel-filtration chromatography

The quaternary conformation of FαB and PαB was analyzed by analytical gel-filtration chromatography. The estimated molecular mass of FαB was 450 kDa, which was

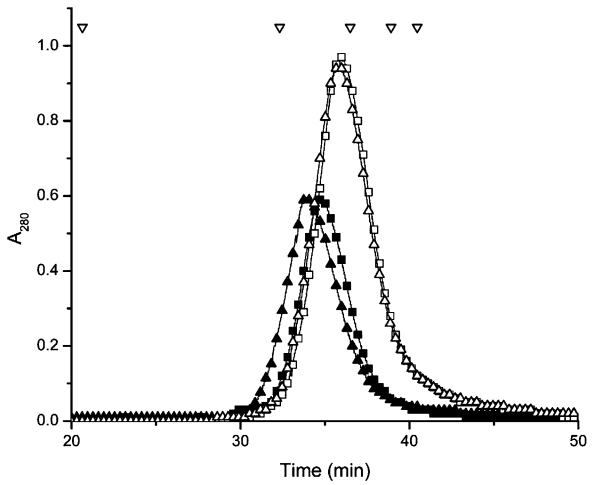

Fig. 8. Analytical gel-filtration analysis of the recombinant FαB and PαB. The molecular masses for FαB (□), 60°C preheated FαB (△), PαB (■) and 50°C preheated PαB (▲) were 450, 450, 550 and 580 kDa, respectively. The width-of-half-height in volume of FαB, 60°C preheated FαB, PαB and 50°C preheated PαB were 1·5, 1·5, 1·3 and 1·3 ml, respectively. The symbols (▽) indicate the elution time of molecular-mass standards, 1, blue dextran (~2000 kDa); 2, bovine thyroglobulin (669 kDa); 3, horse spleen apoferritin (443 kDa); 4, sweet potato β-amylase (200 kDa); 5, yeast alcohol dehydrogenase (150 kDa).

smaller than PαB (550 kDa) but the width-of-half-height (volume) of FαB (1·5 ml) was larger than PαB (1·3 ml) (Fig. 8). Therefore, FαB is more dispersed than PαB regarding its aggregation state. It indicated that FαB possesses a larger size distribution than PαB. After preheating for 30 min, we found that FαB could maintained its oligomerization as non-preheated FαB after preheating treatment at 60°C; however, PαB preheated at 50°C possessed a larger molecular mass (580 kDa) than non-preheated PαB but with a similar width-of-half-height (Fig. 8). Thus, preheating treatment increases the molecular size of PαB without affecting its size distribution but no effects on the molecular size and size distribution of FαB. Similar preheating effect on molecular mass of PαB was also found in human αB-crystallin (Sun and Liang, 1998). These results indicated that the refolding of FαB after preheating treatment is better than PαB.

3.8. Analytical ultracentrifugation

In order to obtain hydrodynamic information about the size and shape of αB-crystallin, FαB and PαB were analyzed by the sedimentation velocity in an analytical ultracentrifuge. Continuous sedimentation coefficient analysis of the sedimentation data was analyzed by the SEDFIT program (Schuck, 2000) (Fig. 9). The A−C plots shown in Fig. 9 indicated that the fitting results were consistent and reliable. The curves of αB-crystallins revealed a polydisperse system with a broad distribution of different size species similar to our previous report (Liao et al., 2002a). The sedimentation coefficient (*S*) of the FαB was about 12*S*,

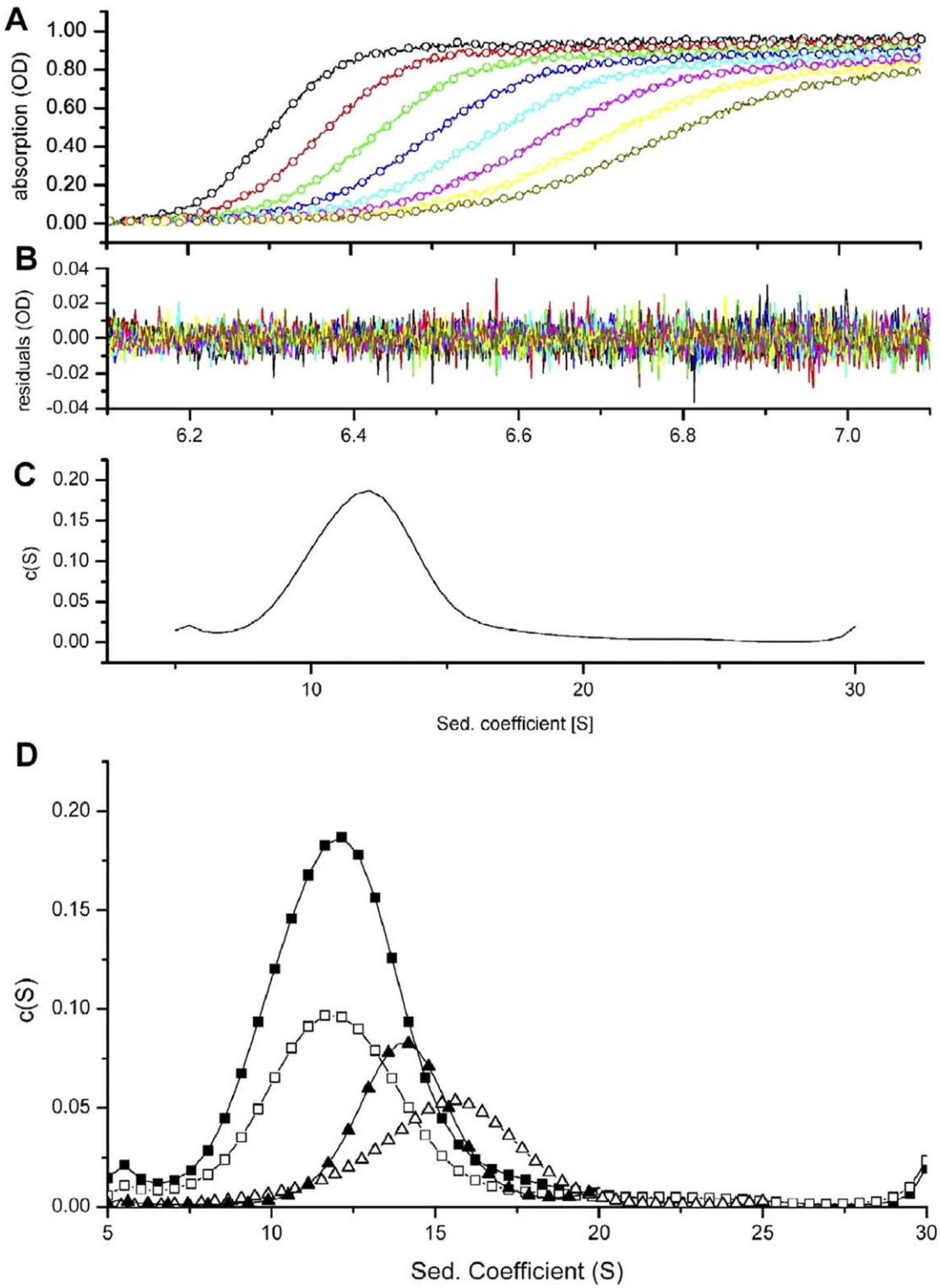

Fig. 9. Analytical ultracentrifugation analysis of FαB and PαB. (A) Trace of absorbance at 280 nm during sedimentation (line) and from fitted data (circle) of non-preheated FαB. (B) Fitting residuals of the data shown in (A). (C) Continuous $c(S)$ plot of the analyzed result from (A). (D) Comparison of $c(S)$ plots for the FαB (■), FαB preheated at 60°C (□), PαB (▲), and PαB preheated at 50°C (△). The sedimentation coefficient (S) of the native and preheated FαB and PαB were 12S, 12S, 14·5S and 15·5S, respectively.

which was smaller than PαB (14·5S) (Fig. 9(D)). The data are compatible with the gel-filtration results (Fig. 8) that FαB is smaller in size than PαB. The sedimentation coefficient (S) of the FαB preheated at 60°C is the same as non-preheated FαB and PαB preheated at 50°C possesses a larger S value (15·5S) than non-preheated PαB, which are compatible to the results of gel-filtration after preheating treatment.

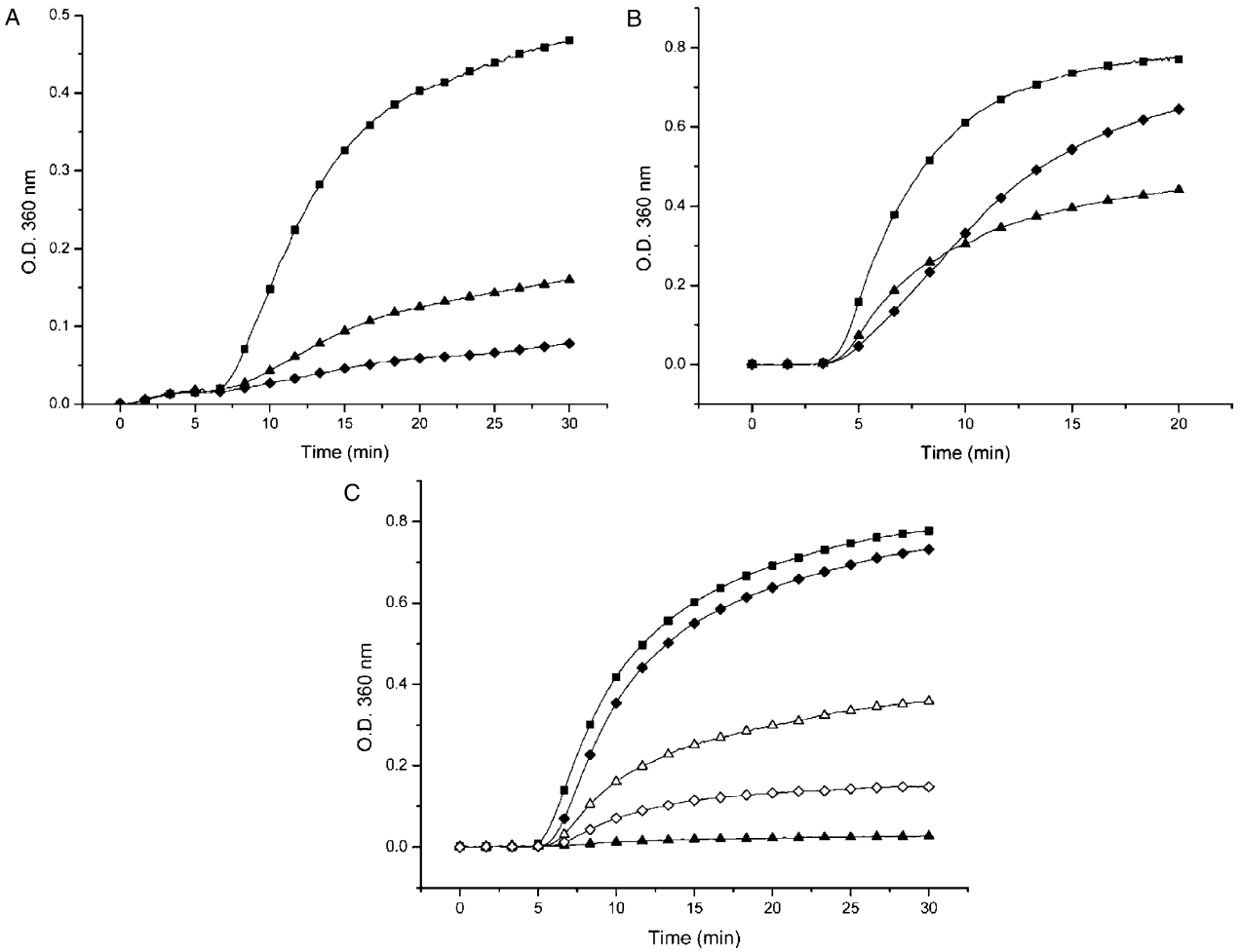

Fig. 10. Comparison of chaperone-like activity between FαB and PαB. (A) ADH aggregation at 50°C with a molar ratio of 2:1 (ADH/αB-crystallin), (■), ADH alone; (▲), ADH plus FαB; (◆), ADH plus PαB. (B) ADH aggregation at 60°C with a molar ratio of 2:1 (ADH/αB-crystallin), (■), ADH alone; (▲), ADH plus FαB; (◆), ADH plus PαB. (C) Insulin aggregation at 37°C, (■), insulin only; (▲), insulin plus FαB with a molar ratio of 28:1 (insulin/αB-crystallin); (△), insulin plus FαB with a molar ratio of 56:1; (◆), insulin plus PαB with a molar ratio of 28:1; (◇), insulin plus PαB with a molar ratio of 7:1. It is noted that FαB at a much lower chaperone/substrate ratio of 1:28 can completely inhibit DTT-induced insulin aggregation than PαB (1:7).

Both results from gel-filtration and analytical ultracentrifugation indicate that FαB possesses better refolding potential than PαB.

3.9. Comparison of chaperone-like activity

The chaperone-like activities of FαB and PαB against thermal aggregation were performed by using ADH as substrate at 50 (Fig. 10(A)) and 60°C (Fig. 10(B)). At a molar ratio of 2:1 (ADH/αB-crystallins), the suppression of ADH aggregation at 50°C by PαB (about 83%) was better than FαB (about 66%). The data are consistent with the ANS-binding experiments (Fig. 7(B)), showing that α-crystallin with more hydrophobic surface possesses better chaperone-like activity (Raman and Rao, 1994). However, even though FαB was less hydrophobic as revealed by its lower I_{ANS} than PαB at 60°C (Fig. 7(B)), FαB possessed better chaperone-like activity than the PαB (about 43 versus 16%) (Fig. 10(B)). The contradictory data obtained for assays at two different temperatures might be accounted for by the instability of PαB at 60°C (Liao et al., 2002a,b) (Fig. 5). These data also suggest that FαB is more thermostable than PαB.

Reduction of disulfide linkage between insulin A and B chains leads to the aggregation of the B chains (Sanger, 1949). The aggregation could be suppressed by α-crystallin (Farahbakhsh et al., 1995). The chaperone-like activities of FαB and PαB were also analyzed by DTT-induced insulin aggregation (Fig. 10(C)). It was surprising to find that PαB could not prevent DTT-induced insulin aggregation at 25°C with a molar ratio of 28:1 (insulin/αB-crystallin) in contrast to 32% protective ability observed for FαB (data not shown). At 37°C and a molar ratio of 28:1 (insulin/αB-crystallin), FαB could totally prevent the insulin aggregation induced by DTT, however, PαB had just about 6% chaperone-like activity (Fig. 10(C)). At a molar ratio of 56:1, FαB still possessed 54% chaperone-like activity while PαB possessed 81% chaperone-like activity only at a high molar ratio of 7:1 (Fig. 10(C)). These data indeed suggest that FαB possesses

abnormally higher chaperone-like activity than PαB in the DTT-induced insulin aggregation, even though PαB possesses larger surface hydrophobic regions than FαB at 25 and 37°C (Fig. 7(B)).

There is no reason why the two methods should give identical results, even though most reports in the literature imply that the two methods (heat-induced ADH aggregation and DTT-induced insulin aggregation) should provide the same results (Plater et al., 1996; Horwitz et al., 1998b; Lindner et al., 1998) In contrast to the chaperone-like activity to prevent heat-induced protein aggregation (Rao et al., 1993; Raman and Rao, 1994), there is no mechanistic basis to correlate surface hydrophobicity with the chaperone-like activity against chemical denaturation, such as DTT-induced insulin aggregation.

4. Conclusion

In this report, we have cloned, expressed and characterized FαB. The comparison between FαB and PαB was carried out regarding their thermostability, protein conformation and chaperone-like activity. cDNAs of FαB gene was constructed from catfish lenses in order to aid in the genomic analysis of αB-crystallin. The structure–function characterization of FαB bears special biological significance because it belongs to an authentic member of the sHSPs family with chaperone-like activity. FαB possesses higher structural stability than PαB as judged by thermostability measurements (Fig. 5), secondary structure predictions based on CD measurements (Fig. 6), and chaperone-like activity by suppression of ADH aggregation at 60°C (Fig. 10(B)). The distinct properties found in FαB in contrast to most mammalian homologous αB-crystallins coupled with detailed sequence information will provide some deeper insights in the elucidation of structure–function relationship of α-crystallin, and the mechanism underlying crystallin thermostability and the accompanying chaperone-like activity in the near future. Site-specific mutagenesis of FαB on several putative essential sites for αB-crystallin thermostability and chaperone-like activity is currently in progress.

Acknowledgements

This work was supported in part by Academia and the National Science Council (NSC Grants 89-2311-B-002-098, 90-2311-B-002-022 and 91-2311-B-002-015 to S.-H. Chiou), Taipei, Taiwan. We thank Dr P.-Y. Chan for reading and detailed discussion on the manuscript before submission. This report will be submitted as part of a dissertation by C.-M.Y. to Graduate Institute of Life Sciences, National Defense Medical Center in partial fulfilment of the PhD degree.

References

Bloemendal, M., Toumadje, A., Johnson Jr, W.C., 1999. Bovine lens crystallins do contain helical structure: a circular dichroism study. Biochim. Biophys. Acta 1432, 234–238.

Chervitz, S.A., Aravind, L., Sherlock, G., Ball, C.A., Koonin, E.V., Dwight, S.S., Harris, M.A., Dolinski, K., Mohr, S., Smith, T., Weng, S., Cherry, J.M., Botstein, D., 1998. Comparison of the complete protein sets of worm and yeast: orthology and divergence. Science 282, 2022–2028.

Chiesa, R., Gawinowicz-Kolks, M.A., Kleiman, N.J., Spector, A., 1987. The phosphorylation sites of the B2 chain of bovine α-crystallin. Biochem. Biophys. Res. Commun. 144, 1340–1347.

Chiou, S.H., 1986. Phylogenetic comparison of lens crystallins from the vertebrate and invertebrate-convergent or divergent evolution? FEBS Lett. 201, 69–73.

Chiou, S.H., Chang, T., Chang, W.C., Kuo, J., Lo, T.B., 1986. Characterization of lens crystallins and their mRNA from the carp lenses. Biochim. Biophys. Acta 871, 324–328.

de Jong, W.W., Hendriks, W., 1986. The eye lens crystallins: ambiguity as evolutionary strategy. J. Mol. Evol. 24, 121–129.

Demeler, B., Saber, H., 1998. Determination of molecular parameters by fitting sedimentation data to finite-element solutions of the Lamm equation. Biophys. J. 74, 444–454.

Dinner, A.R., Sali, A., Smith, L.J., Dobson, C.M., Karplus, M., 2000. Understanding protein folding via free-energy surfaces from theory and experiment. Trends Biochem. Sci. 25, 331–339.

Farahbakhsh, Z.T., Huang, Q.L., Ding, L.L., Altenbach, C., Steinhoff, H.J., Horwitz, J., Hubbell, W.L., 1995. Interaction of α-crystallin with spin-labeled peptides. Biochemistry 34, 509–516.

Gill, S.C., von Hippel, P.H., 1989. Calculation of protein extinction coefficients from amino acid sequence data. Anal. Biochem. 182, 319–326.

Golenhofen, N., Ness, W., Wawrousek, E.F., Drenckhahn, D., 2002. Expression and induction of the stress protein αB-crystallin in vascular endothelial cells. Histochem. Cell Biol. 117, 203–209.

Groenen, P.J., Merck, K.B., de Jong, W.W., Bloemendal, H., 1994. Structure and modifications of the junior chaperone α-crystallin. From lens transparency to molecular pathology. Eur. J. Biochem. 225, 1–19.

Harpaz, Y., Gerstein, M., Chothia, C., 1994. Volume changes on protein folding. Structure 2, 641–649.

Hein, J., 1990. Unified approach to alignment and phylogenies. Methods Enzymol. 183, 626–645.

Hendrick, J.P., Hartl, F.U., 1993. Molecular chaperone functions of heat-shock proteins. Ann. Rev. Biochem. 62, 349–384.

Higgins, D.G., Bleasby, A.J., Fuchs, R., 1991. CLUSTAL V: improved software for multiple sequence alignment. CABIOS 5, 151–153.

Horwitz, J., 1992. α-Cystallin can function as a molecular chaperone. Proc. Nat. Acad. Sci. USA 89, 10449–10453.

Horwitz, J., 1993. Proctor lecture. The function of α-crystallin. Invest. Ophthalmol. Vis. Sci. 34, 10–22.

Horwitz, J., Huang, Q.L., Ding, L., Bova, M.P., 1998a. Lens α-crystallin: chaperone-like properties. Methods Enzymol. 290, 365–383.

Horwitz, J., Bova, M., Huang, Q.L., Ding, L., Yaron, O., Lowman, S., 1998b. Mutation of αB-crystallin: effects on chaperone-like activity. Int. J. Biol. Macromol. 22, 263–269.

Ingolia, T.D., Craig, E.A., 1982. Four small Drosophila heat-shock proteins are related to each other and to mammalian α-crystallin. Proc. Nat. Acad. Sci. USA 79, 2360–2364.

Iwaki, T., Kume-Iwaki, A., Liem, R.K., Goldman, J.E., 1989. αB-Cystallin is expressed in non-lenticular tissues and accumulates in Alexander's disease brain. Cell 57, 71–78.

Jackson, M., Gentleman, S., Lennox, G., Ward, L., Gray, T., Randall, K., Morrell, K., Lowe, J., 1995. The cortical neuritic pathology of Huntington's disease. Neuropathol. Appl. Neurobiol. 21, 18–26.

Johnson, J.D., El-Bayoumi, M.A., Weber, L.D., Tulinsky, A., 1979. Interaction of α-chymotrypsin with the fluorescent probe 1-anilino-naphthalene-8-sulfonate in solution. Biochemistry 18, 1292–1296.

Klemenz, R., Frohli, E., Steiger, R.H., Schafer, R., Aoyama, A., 1991. αB-Cystallin is a small heat-shock protein. Proc. Nat. Acad. Sci. USA 88, 3652–3656.

Kyte, J., Doolittle, R.F., 1982. A simple method for displaying the hydropathic character of a protein. J. Mol. Biol. 157, 105–132.

Liang, J.J., Sun, T.X., Akhtar, N.J., 1999. Spectral contribution of the individual tryptophan of αB-crystallin: a study by site-directed mutagenesis. Protein Sci. 8, 2761–2764.

Liao, J.H., Hung, C.C., Lee, J.S., Wu, S.H., Chiou, S.H., 1998. Characterization, cloning, and expression of porcine αB-crystallin. Biochem. Biophys. Res. Commun. 244, 131–137.

Liao, J.H., Lee, J.S., Chiou, S.H., 2002a. C-terminal lysine truncation increases thermostability and enhances chaperone-like function of porcine αB-crystallin. Biochem. Biophys. Res. Commun. 297, 309–316.

Liao, J.H., Lee, J.S., Chiou, S.H., 2002b. Distinct roles of αA- and αB-crystallins under thermal and UV stresses. Biochem. Biophys. Res. Commun. 295, 854–861.

Lindner, R.A., Kapur, A., Mariani, M., Titmuss, S.J., Carver, J.A., 1998. Structural alterations of α-crystallin during its chaperone action. Eur. J. Biochem. 258, 170–183.

Logsdon Jr, J.M., 1998. The recent origins of spliceosomal introns revisited. Curr. Opin. Genet. Dev. 8, 637–648.

Mattick, J.S., Gagen, M.J., 2001. The evolution of controlled multitasked gene networks: the role of introns and other non-coding RNAs in the development of complex organisms. Mol. Biol. Evol. 18, 1611–1630.

Merck, K.B., De Haard-Hoekman, W.A., Oude Essink, B.B., Bloemendal, H., De Jong, W.W., 1992. Expression and aggregation of recombinant αA-crystallin and its two domains. Biochim. Biophys. Acta 1130, 267–276.

Perng, M.D., Muchowski, P.J., van Den, I.P., Wu, G.J., Hutcheson, A.M., Clark, J.I., Quinlan, R.A., 1999. The cardiomyopathy and lens cataract mutation in αB-crystallin alters its protein structure, chaperone activity, and interaction with intermediate filaments in vitro. J. Biol. Chem. 274, 33235–33243.

Perry, R.E., Abraham, E.C., 1986. High-performance liquid chromatographic separation of lens crystallins and their subunits. J. Chromatogr. 351, 103–110.

Plater, M.L., Goode, D., Crabbe, M.J., 1996. Effects of site-directed mutations on the chaperone-like activity of αB-crystallin. J. Biol. Chem. 271, 28558–28566.

Posner, M., Kantorow, M., Horwitz, J., 1999. Cloning, sequencing and differential expression of αB-crystallin in the zebrafish, *Danio rerio*. Biochim. Biophys. Acta 1447, 271–277.

Powers, D.A., 1989. Fish as model systems. Science 246, 352–358.

Raman, B., Rao, C.M., 1994. Chaperone-like activity and quaternary structure of α-crystallin. J. Biol. Chem. 269, 27264–27268.

Rao, P.V., Horwitz, J., Zigler Jr, J.S., 1993. α-Cystallin, a molecular chaperone, forms a stable complex with carbonic anhydrase upon heat denaturation. Biochem. Biophys. Res. Commun. 190, 786–793.

Renkawek, K., de Jong, W.W., Merck, K.B., Frenken, C.W., van Workum, F.P., Bosman, G.J., 1992. αB-Cystallin is present in reactive glia in Creutzfeldt-Jakob disease. Acta Neuropathol. (Berl.) 83, 324–327.

Renkawek, K., Voorter, C.E., Bosman, G.J., van Workum, F.P., de Jong, W.W., 1994. Expression of αB-crystallin in Alzheimer's disease. Acta Neuropathol. (Berl.) 87, 155–160.

Roest Crollius, H., Jaillon, O., Bernot, A., Dasilva, C., Bouneau, L., Fischer, C., Fizames, C., Wincker, P., Brottier, P., Quetier, F., Saurin, W., Weissenbach, J., 2000. Estimate of human gene number provided by genome-wide analysis using *Tetraodon nigroviridis* DNA sequence. Nat. Genet. 25, 235–238.

Rubin, G.M., Yandell, M.D., Wortman, J.R., Gabor Miklos, G.L., Nelson, C.R., Hariharan, I.K., Fortini, M.E., Li, P.W., Apweiler, R., Fleischmann, W., Cherry, J.M., Henikoff, S., Skupski, M.P., Misra, S., Ashburner, M., Birney, E., Boguski, M.S., Brody, T., Brokstein, P., Celniker, S.E., Chervitz, S.A., Coates, D., Cravchik, A., Gabrielian, A., Galle, R.F., Gelbart, W.M., George, R.A., Goldstein, L.S., Gong, F., Guan, P., Harris, N.L., Hay, B.A., Hoskins, R.A., Li, J., Li, Z., Hynes, R.O., Jones, S.J., Kuehl, P.M., Lemaitre, B., Littleton, J.T., Morrison, D.K., Mungall, C., O'Farrell, P.H., Pickeral, O.K., Shue, C., Vosshall, L.B., Zhang, J., Zhao, Q., Zheng, X.H., Lewis, S., 2000. Comparative genomics of the eukaryotes. Science 287, 2204–2215.

Sanger, F., 1949. Fractionation of oxidized insulin. Biochem. J. 44, 126–128.

Schuck, P., 2000. Size-distribution analysis of macromolecules by sedimentation velocity ultracentrifugation and lamm equation modeling. Biophys. J. 78, 1606–1619.

Sreerama, N., Venyaminov, S.Y., Woody, R.W., 1999. Estimation of the number of α-helical and β-trand segments in proteins using circular dichroism spectroscopy. Protein Sci. 8, 370–380.

Sun, T.X., Liang, J.J., 1998. Intermolecular exchange and stabilization of recombinant human αA- and αB-crystallin. J. Biol. Chem. 273, 286–290.

van der Ouderaa, F.J., de Jong, W.W., Bloemendal, H., 1973. The amino-acid sequence of the αA2 chain of bovine α-crystallin. Eur. J. Biochem. 39, 207–222.

van der Ouderaa, F.J., De Jong, W.W., Hilderink, A., Bloemendal, H., 1974. The amino-acids sequence of the αB2 chain of bovine α-crystallin. Eur. J. Biochem. 49, 157–168.

Vicart, P., Caron, A., Guicheney, P., Li, Z., Prevost, M.C., Faure, A., Chateau, D., Chapon, F., Tome, F., Dupret, J.M., Paulin, D., Fardeau, M., 1998. A missense mutation in the αB-crystallin chaperone gene causes a desmin-related myopathy. Nat. Genet. 20, 92–95.

Wistow, G., 1985. Domain structure and evolution in α-crystallins and small heat-shock proteins. FEBS Lett. 181, 1–6.

Wistow, G.J., Piatigorsky, J., 1988. Lens crystallins: the evolution and expression of proteins for a highly specialized tissue. Ann. Rev. Biochem. 57, 479–504.